M.S. Dissertation

Analysis of plasma-treated sapphire surface and its effect on crystallized Al_2O_3 quality

플라즈마 처리가 사파이어 기판 표면과 결정화된 알루미나의 결정성에 미치는 영향 분석

2018년 2월

서울대학교 대학원

재료공학부

김 기 웅

Abstract

Analysis of plasma-treated sapphire surface and its effect on crystallized Al_2O_3 quality

Giwoong Kim

Department of Materials Science and Engineering

College of Engineering

Seoul National University

GaN-based LEDs, which are a group III-nitride compound semiconductors, are emerging as next-generation lighting technologies due to their superior energy efficiency and loger luminescent life than conventional incandescent lamps and fluorescent lamps. Generally, a GaN-based compound semiconductors are grown on a sapphire substrate by a hetero-epiaxy. However, there are problem of high threading dislocation density due to lattice constant

mismatch, wafer bow due to difference in the thermal expansion coefficients between substrate and GaN film, and the low light extraction efficiency due to difference in the refractive index. In order to improve these problems, researches have been carried out to insert a patterns on the sapphire substrate surface to enable lateral overgrowth of GaN film and increase diffuse reflection. Our research group has also developed a CES (cavity-engineered sapphire substrate) which inserts an air cavity arrays on a sapphire substrate surface. When GaN film is grown on a CES, the threading dislocation density decreased due to lateral overgrowth, and the light extraction efficiency increased because of the diffuse reflection. Also, the air cavity arrays reduce the stress inside the thin film, thereby reducing the wafer bow phenomenon.

The CES is fabricated by crystallization of alpha-alumina through thermal treatment of amorphous-alumina deposited on a sapphire substrate. Therefore, in order to obtain a high-quality GaN film, the crystallinity of alumina layer is important. During the CES fabrication process, plasma treatment is performed before depositing the amorphous-alumina layer to remove the PR residue after the photolithography process and to obtain the desired shape pattern. This study was conducted to analyze the effect of plasma treatment on the surface of the sapphire substrate and the crystallinity of the crystallized alumina.

Plasma treatment was performed by adjusting parameters. In this study, plasma treatment was carried out using oxygen (O_2) and argon (Ar) gas. Also, experiments were conducted by controlling the power applied to the plate which the substrate is placed. Fluorine (F) impurities were detected in both the oxygen and argon plasma treatment and about 1% of argon impurities were detected in the case of argon plasma treatment. The oxygen ratio on the surface of the sapphire substrate was increased during the oxygen plasma treatment, and the opposite result was obtained in the case of the argon plasma treatment. Also, as the plate power increases, the stoichiometry of the sapphire substrate surface became more broken. As a result of analysis using AFM technique, the surface morphology and roughness of plasma-treated samples did not much change much, but the crystallized samples showed that nano-sized grains appeared on the surface, and the surface roughness also increased greatly. As a result of the crystallinity analysis, the crystallinity of both gamma-alumina and alpha-alumina was degraded in comparison with the samples that not plasma-treated. Therefore, this study can be used to experminetally examine the effect of plasma treatment on the sapphire substrate surface and the crystallized alumina.

Key Words:

Light emitting diode (LED), GaN, Cavity-engineered sapphire substrate (CES), alumina (Al_2O_3), Solid-phase-epitaxy (SPE), Plasma treatment, Crystallinity

Student Number: 2015-20802

Contents

Abstract ..... **i**

Contents ..... **v**

List of Tables ..... **vii**

List of Figures ..... **viii**

Chapter 1. Introduction **1**

1.1. Background theory 1
1.1.1. GaN-based LEDs 1
1.1.2. Technical issues in GaN-based LEDs 4

1.2. Cavity Engineered Sapphire substrate (CES) 9
1.2.1. Advantages of CES 9
1.2.2. Fabrication process of CES 11
1.2.3. Necessity of plasma treatment 13
1.2.4. Solid-phase-epitaxy (SPE) of alumina 15

1.3. Purpose of the study 17

Chapter 2. Experimental and analysis tools **19**

2.1 CES fabrication techniques 19
2.1.1 Atomic layer deposition (ALD) 19
2.1.2 Inductively coupled plasma etcher (ICP-etcher) 21

2.2 Characterization techniques 23
2.2.1 Atomic force microscopy (AFM) 23
2.2.2 X-ray photoelectron spectroscopy (XPS) 23
2.2.3 High resolution X-ray diffraction (HR-XRD) 23

Chapter 3. Experimental results and discussion 25

3.1. Experimental setup.....25
3.1.1 Plasma treatment 25
3.1.2 Amorphous alumina deposition.....27
3.1.3 Thermal treatment 29

3.2. AFM analysis (roughness, morphology) 31
3.2.1 Bare sapphire surface 31
3.2.2 Amorphous alumina 31
3.2.3 Crystallized alumina (gamma-phase, alpha-phase) 34
3.2.4 Summary.....37

3.3. XPS analysis (stoichiometry, impurities) 39
3.3.1 Oxygen plasma treated 39
3.3.2 Argon plasma-treated.....41
3.3.3 Summary.....43

3.4. XRD analysis (crystalline quality) 44
3.4.1 Crystallized gamma-phase alumina 44
3.4.2 Crystallized alpha-phase alumina.....46
3.4.3 Summary.....50

Chapter 4. Conclusion.....51

Reference.....52

국 문 초 록 54

Publication list 56

List of Tables

Table 3.1 Plasma treatment conditions in the experiment.....26

List of Figures

Figure1.1 Bandgap energy versus lattice constant of III-V nitride semiconductors at room temperature [1]. 3
Figure1.2 The epitaxy relationship and lattice mismatch between sapphire substrate and GaN thin film [3]. 6
Figure 1.3 Schematic diagram of the wafer bowing process [9]. 7
Figure 1.4 Surface roughening for light scattering [13]. 8
Figure 1.5 Cross-section SEM image of CES (a) Before GaN growth (b) After GaN growth [15]. 10
Figure 1.6 Schematic diagram of CES fabrication process 12
Figure 1.7 (a) Optical microscope (OM) image of surface peeling (b) SEM image of PR pattern array before and after plasma treatment 14
Figure 1.8 Schematic diagram of amorphous alumina crystallization process by SPE [18] 16
Figure 1.9 The schematic of (a) reacation between plasma and substrate surface (b) SPE process on damaged surface of sapphire substrate 18
Figure 2.1 ALD mechanism of amorphous alumina thin layer [19] 20
Figure 2.2 Schematic diagram of ICP-etcher [20] 22
Figure 3.1 Density of amorphous alumina layer versus growth temperature [21]. 28
Figure 3.2 A sequence of thermal treatment for PR calcination and crystallization 30
Figure 3.3 AFM images obtained to measure the sapphire substrate surface morphology and rms rougness depending on plasma treatment conditions. . 32
Figure 3.4 AFM images obtained to measure the amorphous alumina thin layer morphology and rms rougness depending on plasma treatment conditions. . 33
Figure 3.5 2D-AFM images of crystallized alumina (a) gamma-phase (b) alpha-phase 35
Figure 3.6 3D-AFM images of crystallized alumina (a) gamma-phase (b) alpha-phase 36
Figure 3.7 Rms roughness depending on the plate power. 38
Figure 3.8 (a) XPS spectra of oxygen plasma-treated samples (b) table of fluorine concentration and O/Al ratio 40
Figure 3.9 (a) XPS spectra of argon plasma-treated samples (b) table of fluorine

concentration and O/Al ratio 42
Figure 3.10 ω-rocking curve and FWHM values of crystallized gamma-phase alumina (222) plane 45
Figure 3.11 RSM images of sapphire substrate and crystallized alpha-alumina on plasma un-treated sapphire substrate..... 47
Figure 3.12 RSM images of crystallized alpha-alumina on plasma-treated substrate and the table of summarized FWHM data..... 48
Figure 3.13 RSM images of CES and the table of summarized FWHM data. 49

Chapter 1. Introduction

1.1 Background theory

1.1.1 GaN-based LEDs

Recently, Light emitting diodes (LEDs) are widely recognized as light source to replace traditional light bulbs or fluorescent bulbs due to their high efficiency and long life span. In 2014, the Novel Prize in Physics was awarded to three Japanese by invention GaN-based blue LED and it make possible to realize a white LED.The bandgap energy of GaN is 3.4eV at room temperature and emits near-ultraviolet ray (λ=365 nm) [1]. Also, as seen in Figure 1.1, depending on composition of material (In or Al) in GaN, the wavelength of light emitted can be changed. LEDs can be used not only in the visible ray region, but also in ultraviolet and infrared ray region, so the use thereof is very diverse.

Epitaxial growth refers to the growth of a crystalline thin film on a crystalline substrate with the identical or similar crystalline structure. There are two types of epitaxial growth: homoepitaxy and heteroepitaxy. Homoepitaxy refers to a method of growing a thin film of the same material as a substrate, e.g. Si film on Si substrate or GaN film on GaN substrate. Heteroepitaxy refers to a method of growing a thin film of the different material as a substrate, e.g. GaAs film on Si substrate or GaN film on Sapphire substrate. The quality of film grown by homoepitaxy is better than grown by heteroepitaxy. Unfortunately, it is very difficult to make high quality GaN substrate. Therefore, GaN-based LED is mainly fabricated by heteroepitaxy; growing GaN film on single crystal sapphire substrate. There are several technical issues by

using heteroepitaxy, such as high threading dislocation density due to lattice mismatch, wafer bowing by thermal coefficient mismatch and mosaic crystal structure [2]. Studies and experiments to improve these problems have continues to the present.

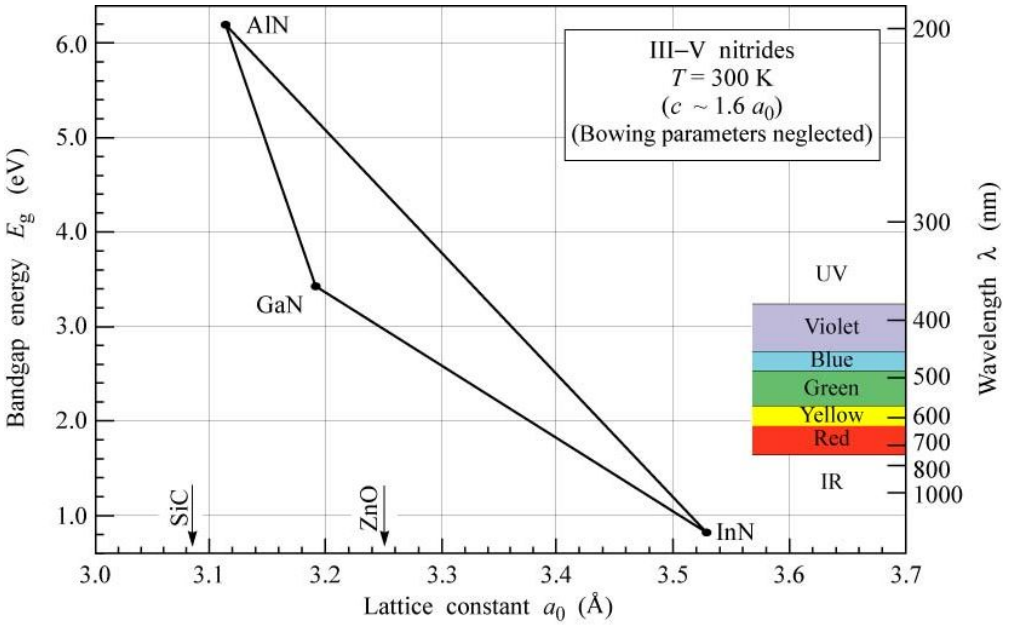

Figure1.1 Bandgap energy versus lattice constant of III-V nitride semiconductors at room temperature [1].

1.1.2 Technical issues in GaN-based LEDs

Despite many advantage of GaN-based LEDs, there are several technical issues in GaN-based LEDs. First issue is high threading dislocation density of GaN thin film. The epitaxial relationship between sapphire substrate and GaN thin film is demonstrated in Figure 1.2 [3]. In GaN/Sapphire hetero-epitaxy structure, a large lattice mismatch (~16.1%) results in high density threading dislocation. Threading dislocations are known as nonradiative recombination centers where the electron-hole recombination is converted to phonons instead of photons [4]. A conventional GaN film grown by metal-organic chemical vapor deposition (MOCVD) has a high threading dislocation density (10^7 - 10^{10} cm^{-2}) [5]. To improve this problem, Epitaxial lateral overgrowth (ELO) method has been widely used [6-7].

Second issue is large thermal coefficient mismatch between sapphire substrate and GaN film. The thermal coefficient mismatch between a-plane sapphire substrate ($7.5x10^{-6}$ K^{-1}) and a-plane GaN film ($5.59x10^{-6}$ K^{-1}) is known about 34% [8]. After GaN film growth at high temperature (1040 ℃) by MOCVD system, the wafer is cooled to room temperature. In this process, the sapphire substrate with larger thermal coefficient shrinks more than GaN film, thereby tensile stress induced to sapphire substrate while compressive stress induces to GaN film. This unbalanced stress causes the wafer to be bent into a convex shape. The schematic diagram of wafer bowing is shown in Figure 1.3 [9]. This wafer bowing situation not only lowers the crystallinity of GaN film but also makes it difficult to fabricate LED device. Furthermore, the larger the wafer size, wafer bowing more heavily up which is an obstacle to mass production of GaN film [10]. To avoid this problem, various studies have been conducted including the use of embedded void [11-12].

Third issue is low light extraction efficiency because of the large refractive index of GaN. The large amount of light waves from the LED to the air is suppressed and reflected by the large refractive index difference between GaN (n_{GaN} = 2.43) and air (n_{air} = 1) know as total internal reflection (TIR). The critical angle (refraction angle = 90°) of GaN/air interface is about 23.5° which is very small value to have high light extraction efficiency. To improve this problem, studies such as roughening the surface to scattering the light (Figure 1.4) [13] or inserting the voids into the GaN film have been continuing [14].

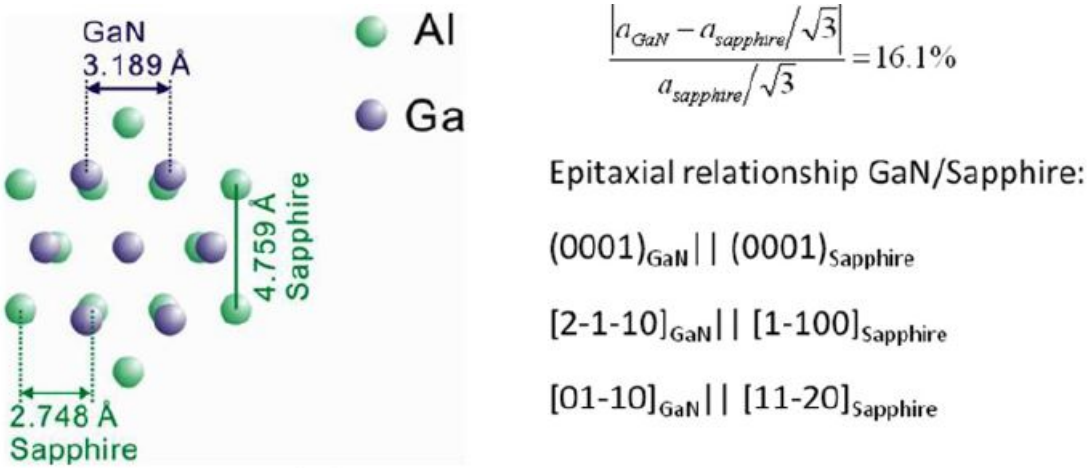

Figure1.2 The epitaxy relationship and lattice mismatch between sapphire substrate and GaN thin film [3].

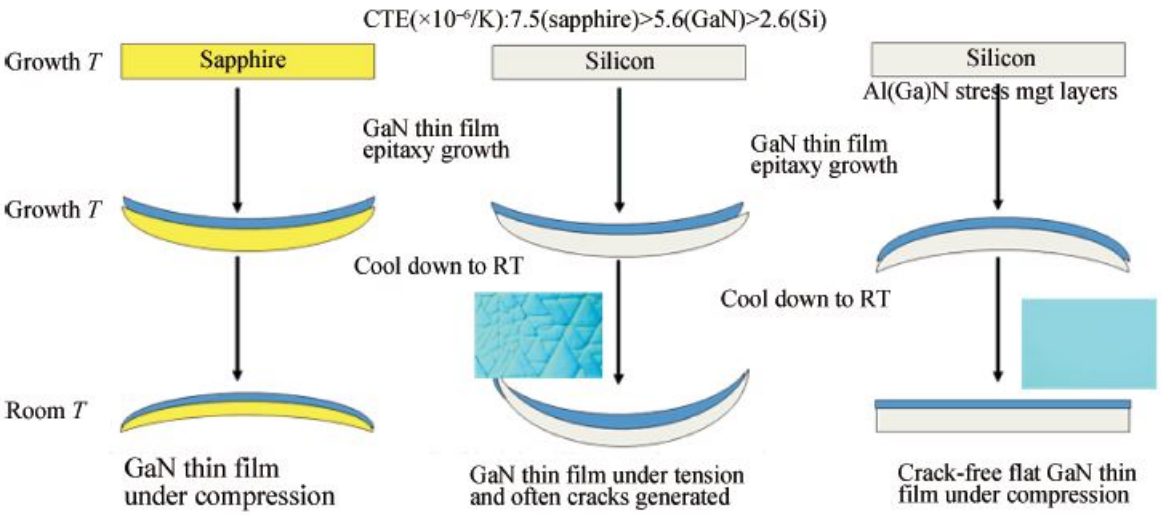

Figure 1.3 Schematic diagram of the wafer bowing process [9].

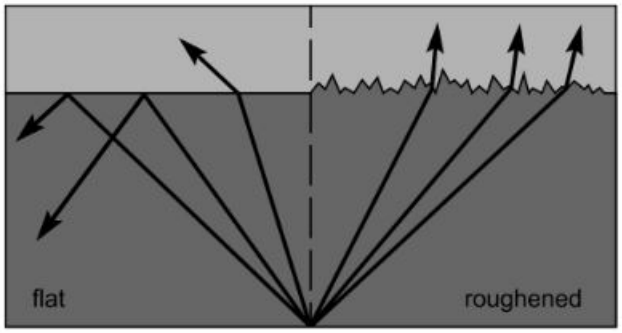

Figure 1.4 Surface roughening for light scattering [13].

1.2 Cavity Engineered Sapphire substrate (CES)

1.2.1 Advantages of CES

Our research group has developed cavity-engineered sapphire substrate (CES) to increase the efiiciency of LED devices. CES is a structure in which air-cavity arrays enclosed by α phase-Al_2O_3 are arranged on a sapphire substrate with regular period. By using air-cavity arrays, we can improve the issues of GaN-based LEDs which mentioned above. During the GaN growth, air-cavity arrays lead to ELO growth and thus lowering the density of threading dislocation about 26% compared to GaN film on planar sapphire substrate. In addition, incorporated air-cavity in GaN film reduced the wafer bowing by ~30% through lessen the stress in GaN film. Light extraction efficiency is also increasing by using CES. The LED device on CES had 2.2 times higher light ouput power than that on planar sapphire substrate [15]. The SEM images of CES are shown in Figure 1.5. One of the important advantages is that the CES can be easily adjusted to the desired shape, dimensions and configuration.

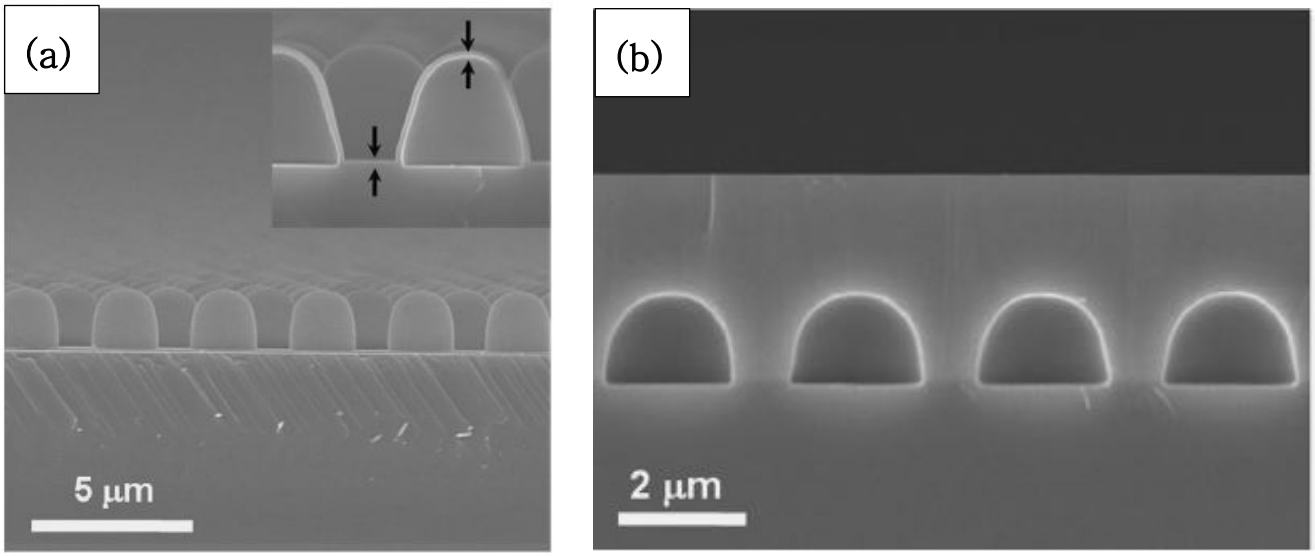

Figure 1.5 Cross-section SEM image of CES (a) Before GaN growth (b) After GaN growth [15].

1.2.2 Fabrication process of CES

The schematic diagram of CES fabrication process is shown in Figure 1.6. First of all, we used conventional photolithography process. A positive photoresist (PR) was coated on 2-inch c-plane sapphire substrate. We used 2.4 μm-diameter, 0.8 μm-space, 2.7 μm-height cylinder shaped PR with hexagonal array. After the PR patterning, additional thermal reflow process by 143 ℃ for 30 mins was conducted to change the shape (cylindrical → hemisphere) of the PR pattern. Then, patterned PR was placed in ICP-etcher system under various process conditions to descum the PR residue and to fabricate the shape of PR that we want. A detailed description of this plasma-treatment process will be coverd in the next chapter. Next, an amorphous alumina (Al_2O_3) film was depositied on the patterned PR by atomic layer deposition (ALD). Then, thermal treatment was performed in air-atmosphere furnace for calcination of PR. During this process, PR is removed by oxidization and only the air-cavity array surrounded by amorphous-alumina shell remains on the substrate surface. After PR calcination, re-deposition of amorphous alumina is performed. Finally, thermal treatment was conducted for crystallization in air-atmosphere furnace. During this annealing process, solid phase epitaxy (SPE) occurred; amorphous alumina was crystallized into metastable γ-phase and then into α-phase. The CES thus fabricated becomes a template for the growth of GaN film.

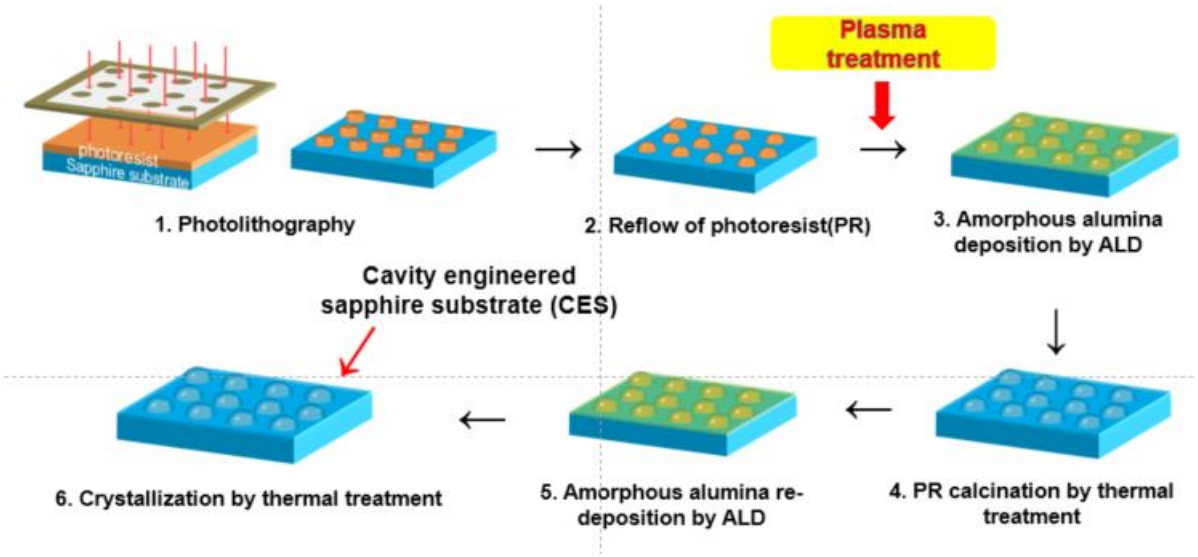

Figure 1.6 Schematic diagram of CES fabrication process

1.2.3 Necessity of plasma treatment

Plasma treatment process is essential for the CES fabrication process for two reasons. The first reason is removal of PR residue. When the thermal treatment is performed after the deposition of amorphous alumina without removing of PR residue, the unintended surface peeling occurs. Figure 1.7 (a) shows the image of surface peeling. The second reson is to get the PR pattern with the desired shape. Figure 1.7 (b) is a SEM image showing the change in shape of PR pattern before and after plasma treatment. Detailed conditions of plasma treatment process will be discussed in later chapter. It can be seen that the shape, size and dimension of the PR pattern change when plasma treatment is performed. Using the optimized plasma treatment condition, we can obtain the PR pattern array what we purpose for. For these two important reasons, plasma treatment process is necessary for the CES fabrication process.

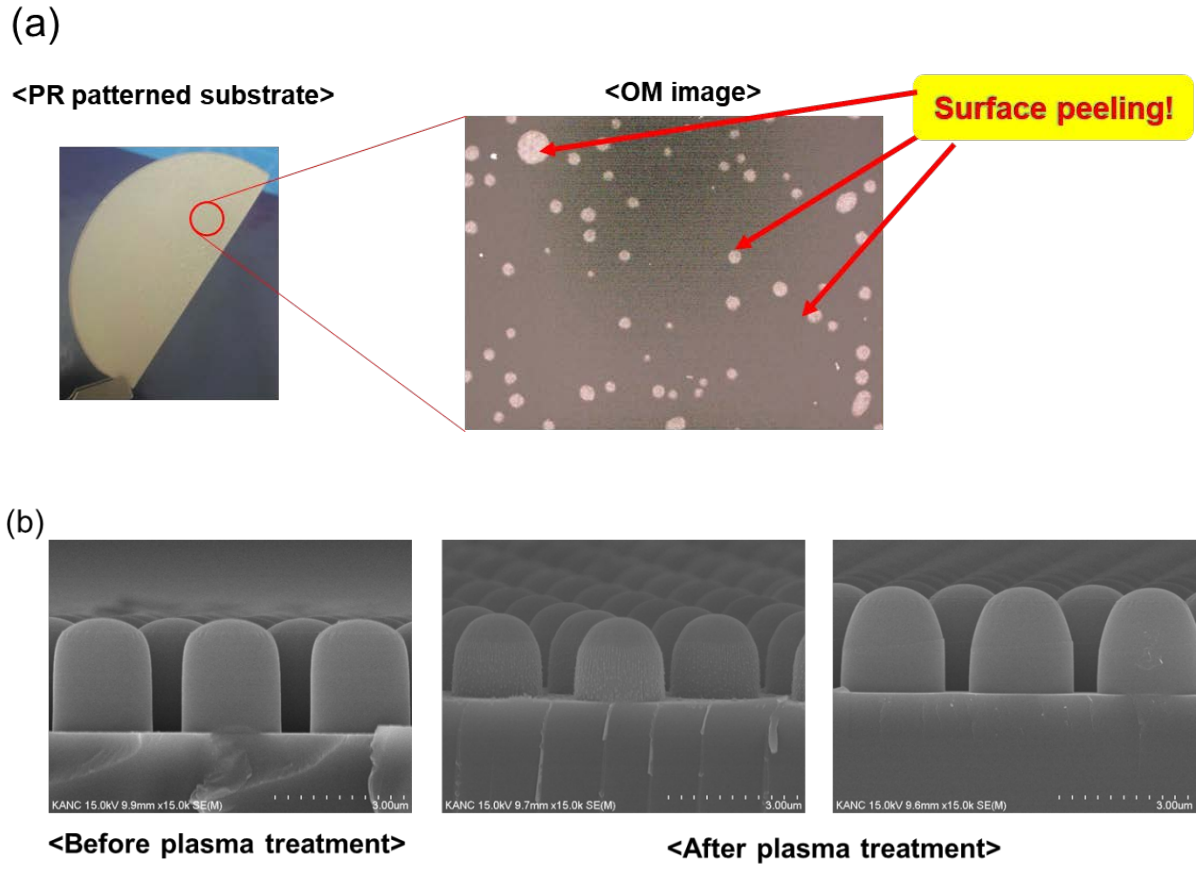

Figure 1.7 (a) Optical microscope (OM) image of surface peeling (b) SEM image of PR pattern array before and after plasma treatment

1.2.4 Solid-phase-epitaxy (SPE) of alumina

Solid-phase-epitaxy (SPE) is that the amorphous layer deposited on single-crystal template crystallizes epitaxially at the interface by rearrangement of atoms [16]. During the crystallization process, amorphous alumina is crystallized through several metastable phases like *delta* and *theta*, whose occurrence may or may not be created [17]. The preferred crystallization of amorphous alumina occurs in two steps from amorphous → gamma → alpha and its schematic diagram is shown in Figure 1.8. In CES fabrication process, amorphous alumina on sapphire substrate is crystallized into a single α-phase alumina during the thermal treatment at the temperature 815 - 1150 ℃. In our previous study, it was confirmed by TEM anlysis that amorphous alumina was crystallized into single α-phase alumina by SPE process under 1100 ℃ for 10 hrs [15].

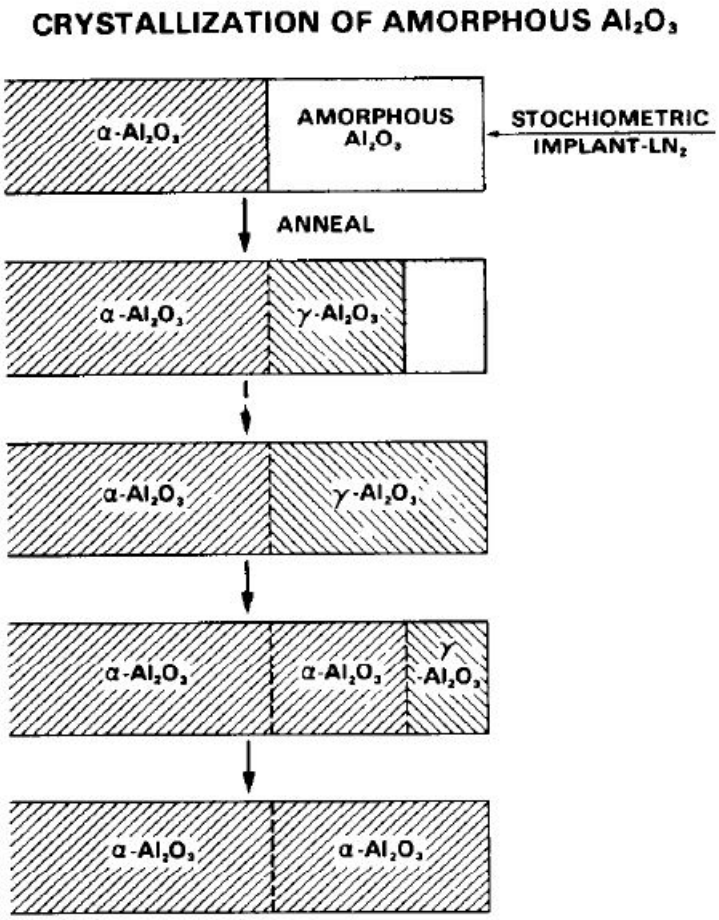

Figure 1.8 Schematic diagram of amorphous alumina crystallization process by SPE [18]

1.3 Purpose of the study

As mentioned above, plasma treatment must be essential for removal of PR residue and shaping the PR pattern. However, it is expected that undesirable problems will occur when plasma treatment proceeds. The radicals and ions generated in the plasma can react with not only the residue of PR but also the surface of the sapphire substrate. Physical and chemical reactions with the substrate surface and the plasma will affect the properties of the substrate. The schematic of plasma treatment process is illustrated in Figure 1.9 (a). The inset shows plasma reactions with the substrate surface. These reactions are believed to roughen the surface and degrade the crystallinity. During the crystallization of the amorphous alumina by SPE process, the crystallization proceeds from the planar region between the patterns. Its schematic diagram is shown in Figure 1.9 (b). Therfore, the crystal quality of this area determins the crystallinity of the CES. Also, the better crystallinity of the CES, the higher quality of GaN film can be obtained.

In this study, we analyze the crystallized alumina on the sapphire substrate with the plasma treatment. This research consists of two major subject: (1) Analysis of the surface morphology of plasma-treated sapphire (2) Analysis of the crystal quality of annealed alumina on plasma-treated sapphire.

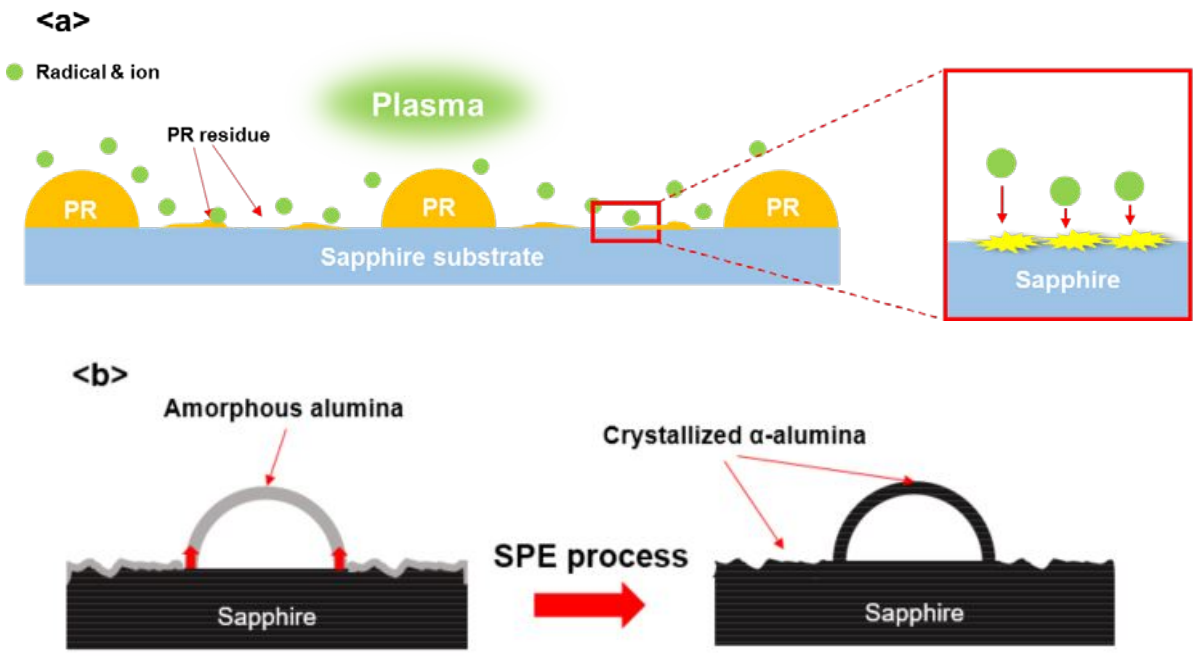

Figure 1.9 The schematic of (a) reacation between plasma and substrate surface (b) SPE process on damaged surface of sapphire substrate

Chapter 2. Experimental and analysis tools

2.1 CES fabrication techniques

2.1.1 Atomic layer deposition (ALD)

Atomic layer deposition (ALD) was used to deposit the thin amorphous alumina layer. Lucida D100 ALD system was utilized for ALD system, using Trimethylaluminum (TMA, $(CH_3)_3Al$) for aluminum precursor and H_2O for oxygen precursor. The deposition process mechanismof ALD is as follows in Figure 2.1. At the first step, a pulse of TMA provides in ALD chamber. Then, reactant TMA bonds to the entire surface of the substrate. After TMA adsorbed layer obtained, high purity nitrogen gas (N_2) purges the byproducts and non-reacted precursor. The pulse and purge step is reapted for the reactant H_2O source. As a result of this one cycle step (TMA pulse → purge → H_2O pulse → purge), one monolayer of amorphous alumina is deposited. Thus, the thickness of layer can be adjusted according to the number of cycles. In this study, pulse time and purge time are 0.2 sec and 3 sec, respectively. Also, the target thickness of amorphous alumina thin layer is about 130 nm.

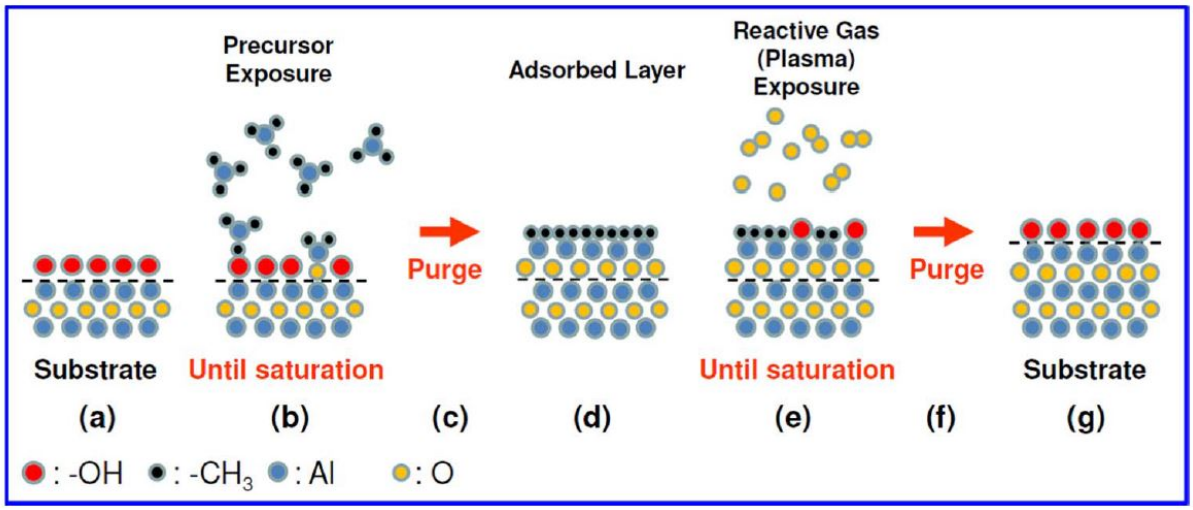

Figure 2.1 ALD mechanism of amorphous alumina thin layer [19]

2.1.2 Inductively coupled plasma etcher (ICP-etcher)

Plasma treatment is conducted by STS Multiplex inductively coupled plasma etcher (ICP-etcher). High-density plasma can be obtained by using ICP-etcher. When an alternating current is supplied to the coil wound around the chamber, an induction magnetic field is formed to accerlerate electrons. ICP-system is widely used as a dry-etching method because it has a high etching rate and asymmetric etching capability. The schematic diagram of ICP-etcher is illustrated in Figure 2.2. The main variables in the plasma process are gas type, mixing ratio, gas flow, plate power, coil power, process time, and so on. In this study, we focused on the effects of gas type and plate power on the sapphire substrate. Because, the reaction mechanism between plasma and substrate varies depending on the type of gas and the plate power has a great influence on the plasma collision energy.

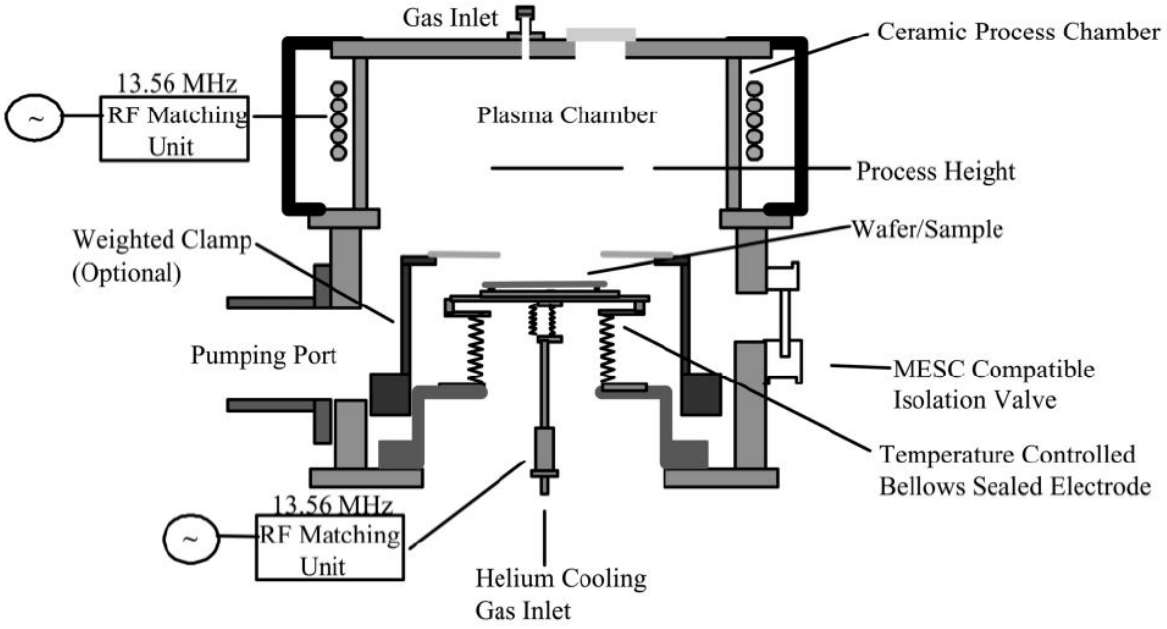

Figure 2.2 Schematic diagram of ICP-etcher [20]

2.2 Characterization techniques

2.2.1 Atomic force microscopy (AFM)

Park Systems XE-100 was used to analysis the roughness and morphology of the sapphire surface. By measuring the van der Waals force acting between the atoms of the sample surface and the probe (silicon-tip), surface morphology can be obtained. The measurement is performed by non-contact mode and XEI program was used for analysis of the raw data.

2.2.2 X-ray photoelectron spectroscopy (XPS)

Kratos AXIS-His was used for quantitative analysis of the sapphire surface. Al Kα (hv=1486.6 eV) was used for X-ray radiation and the base pressure of the chamber is 5×10^{-10} torr. The beam size is 1 mm x 1 mm and the scan depth is under 10 nm. When X-ray is injected on the sample surface, the electrons break the bond and release. Then, the kinetic energy and the number of electrons are measured to obtain the XPS spectra. By using this, we can get chemical state and chemical shift information of the sample surface. For analysis of the XPS spectra, CasaXPS program was used. In this study, we used XPS to observe the impurity atoms and the stoichiometry of the sapphire surface.

2.2.3 High resolution X-ray diffraction (HR-XRD)

Panalytical X'pert pro was used for measuring the crystal quality of the crystallized alumina with an X-ray Cu source operated at 45kV. In this study, we used two method for anlysis (1) ω-rocking curve for gamma alumina (2) reciprocal space mapping (RSM) for alpha alumina.

Chapter 3. Experimental results and discussion

3.1. Experimental setup

3.1.1 Plasma treatment

As mentioned above, we used ICP-etcher for plasma treatment. In this study, we used oxygen (O_2) and argon (Ar) for plasma gas. As is well known, argon plasma only occurs physical reaction and oxygen plasma occurs both chemically and physically with the sample. Since the energy required for plasma generation depends on the ionization energy of the element and there are an optimized values, differet coil powers are applied to the two gases. We flowed coil power 100 W, 800 W for argon plasma and oxygen plasma, respectively. Also, the process time is different for each plasma gas. In the case of argon plasma treatment, only the physical reaction occurs, so that the removal of the PR residue is hard and requires a longer processing time than the oxygen plasma treatment. For similar reason, a large amount of heat is generated in the chuck where the sample is placed due to strong physical collisions. To avoid this, cooling steps was added between the processes during the argon plasma treatment. Generally, the asymmetric etching rate is controlled by changing the plate power. Therefore, the plate power was varied as 0 W, 100 W, 250 W to analyze the effect on the sapphire substrate surface. Table 3.1 shows the summarizing experimental conditions.

Gas	Argon (Ar)	Oxygen (O_2)
Coil power	100 W	800 W
Plate power	0 W, 100 W, 250 W	0 W, 100 W, 250 W
Process time	(20 s processing + 20 s cooling) x 12 times	40 s
Pressure	5 mTorr	5 mTorr
Gas flow	40 sccm	40 sccm

Table 3.1 Plasma treatment conditions in the experiment

3.1.2 Amorphous alumina deposition

As aforementioned, amorphous alumina thin layer was depositied by using ALD. After plasma treatment, alumina deposition was conducted by 2-step (330 cycles at 100 ℃ + 660 cycles at 185 ℃). Also, after PR calcination process, additional deposition was performed with 360 cycles at 185 ℃. The total thickness of alumina layer is about 130 nm. The 2-step ALD technique was developed to reduction of volume contraction during the crystallization due to density increase. The density of amorphous alumina is depending on deposition temperature. Figure 3.1 shows the density of alumina versus growh temperature. Therefore, by adopting 2-step growth, we intend to reduce the difference in density for minimizaing volume contraction.

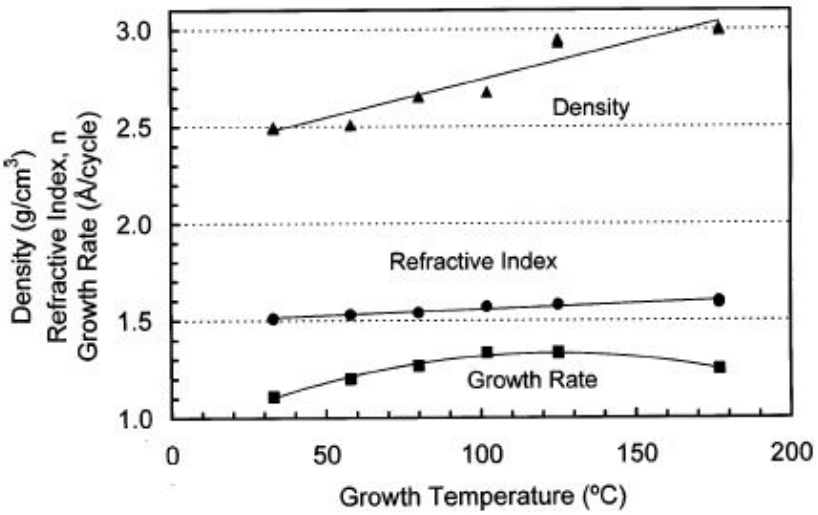

Figure 3.1 Density of amorphous alumina layer versus growth temperature [21]

3.1.3 Thermal treatment

In this study, two thermal treatments were carried out by the air ambient furnace. During the first annealing process (2 hrs at 450 ℃ + 10 hrs at 600 ℃), PR pattern array surrounded by alumina layer is burnt out. Then, the second thermal treatment for crystallization of the alumina is conducted under 4 hrs at 815 ℃ + 7 hrs at 1150 ℃. Phase transformation by SPE occurred from amorphous to gamma phase at 815 ℃ and to alpha phase at 1150 ℃. A sequence of thermal treatment is shown in Figure 3.2.

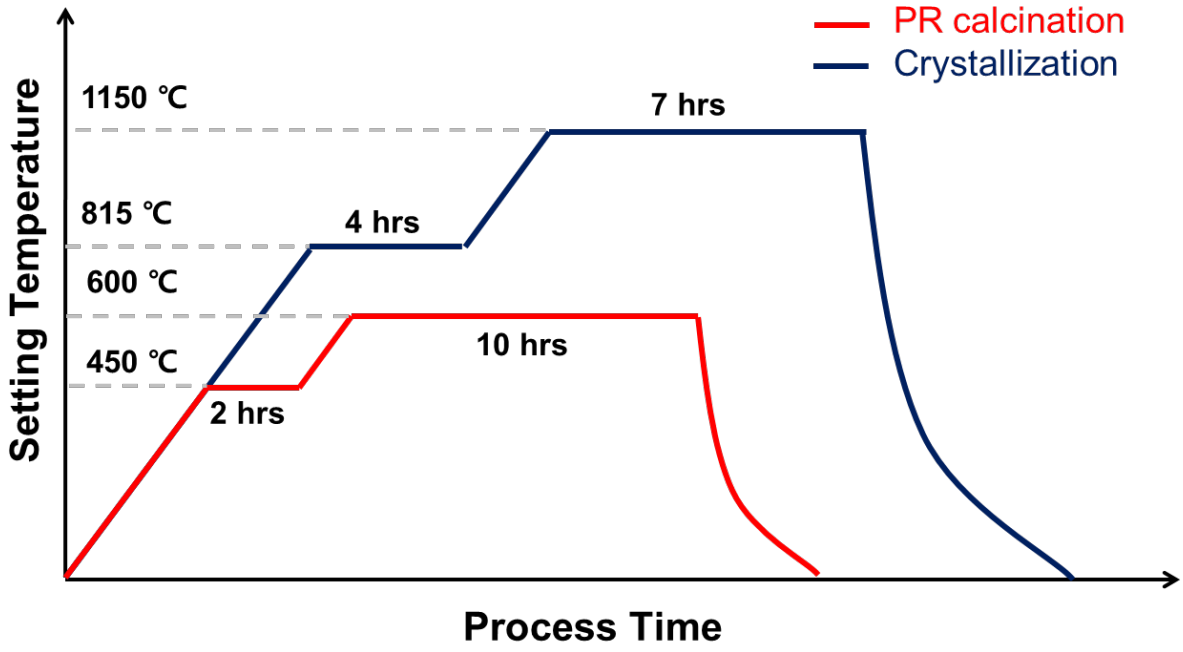

Figure 3.2 A sequence of thermal treatment for PR calcination and crystallization

3.2. AFM analysis (roughness, morphology)

3.2.1 Bare sapphire surface

The surface roughness and morphology of sapphire substarate after plasma treatment were analyzed by AFM technique. Compared to the un-treated sapphire substrate (reference), the treated specimens were prepared by controlling the plasma gas and the plate power, as mentioned in previous chapter. Figure 3.3 exhibits the AFM images of the sapphire surface treated under various plasma conditions. As shown in this figure, there is no significant difference in morphology and root mean square (RMS) rougness with plasma treatment conditions.

3.2.2 Amorphous alumina

The amorphous alumina thin layer deposited on the plasma treated substrate also underwent suface analysis. Figure 3.4 shows the AFM images and rms roughness. The roughness of the reference sample is slightly increased compared to the bare surface. However, as with the above results, there is no significant difference in morphology and rms rougness depending on plasma conditions. Through the AFM analysis, the plasma treatment does not significantly affet the physical morphology change on the surface of substrate.

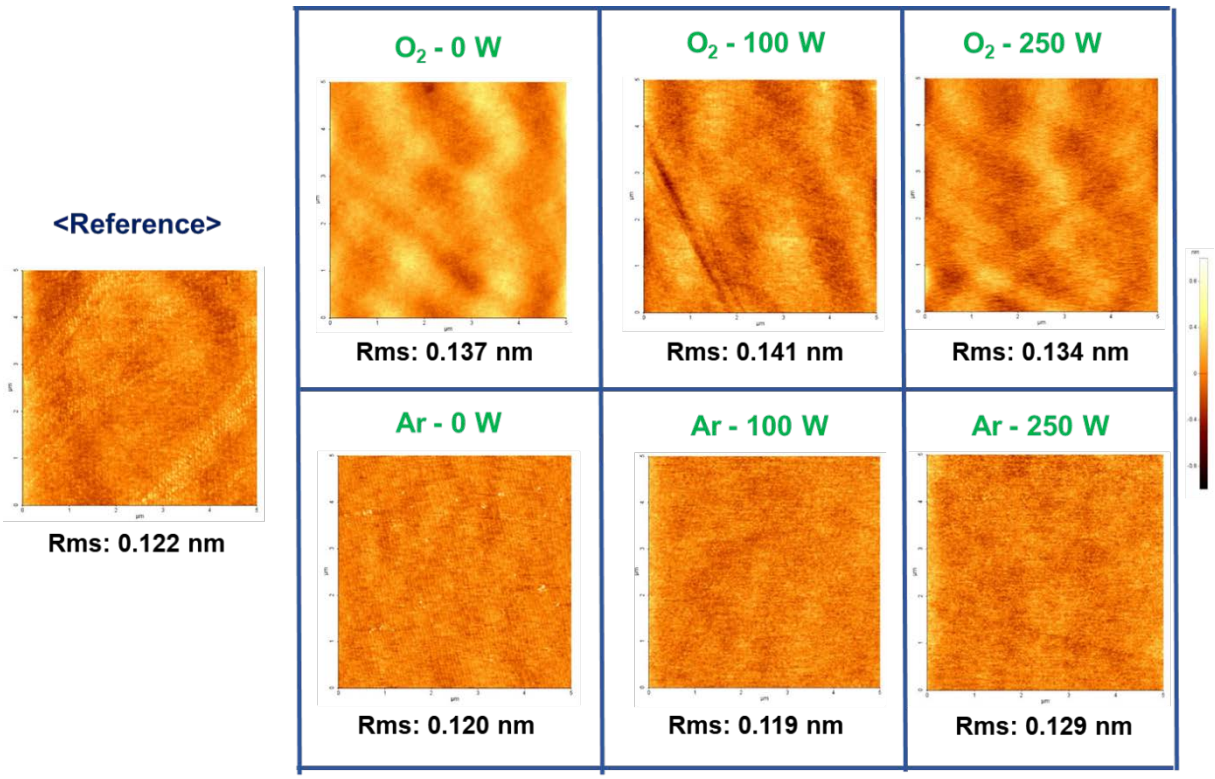

Figure 3.3 AFM images obtained to measure the sapphire substrate surface morphology and rms rougness depending on plasma treatment conditions.

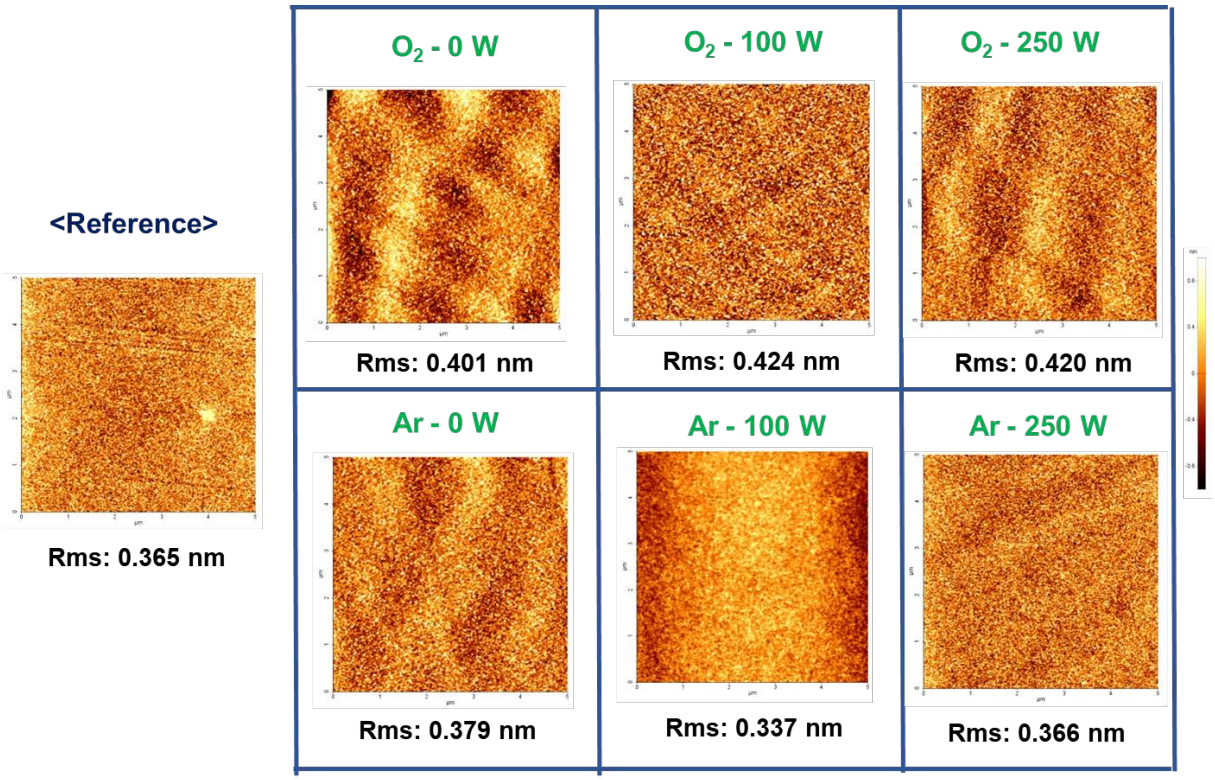

Figure 3.4 AFM images obtained to measure the amorphous alumina thin layer morphology and rms rougness depending on plasma treatment conditions.

3.2.3 Crystallized alumina (gamma-phase, alpha-phase)

After phase transformation by thermal annealing from amorphous to alpha-phase through gamma-phase, the surface morphology and rms roughness were analyzed by AFM techniques. The nano-size grains that were not observed on the bare surface and amorphous-phase alumina were obtained both gamma and the alpha phase. Also, the roughness was greatly increased compared to the reference sample. During the plasma treatment process, the reaction with the substrate surface proceeds, so the stoichiometry of alumina changes and impurities are generated on the surface. As a result, the crystal information on the substrate surface was changed, and the morphology in the alumina thin layer in which the crystallization proceeds has changed by SPE process. In the case of the argon plasam treated samples, the roughness increased more than that of the oxygen plasma treatment, and the morphology seems to be largely changed. This result shows that the argon plasma treatment has a greater effect on the substrate surface than the oxygen plasma treatment. Figure 3.5 shows the 2D-AFM images of the crystallized alumina surface and Figure 3.6 shows the 3D-AFM images. In addition, the morphology of the alpha-phase alumina shows that the crystallization progressed in a direction similar to the gamma-phase morphology.

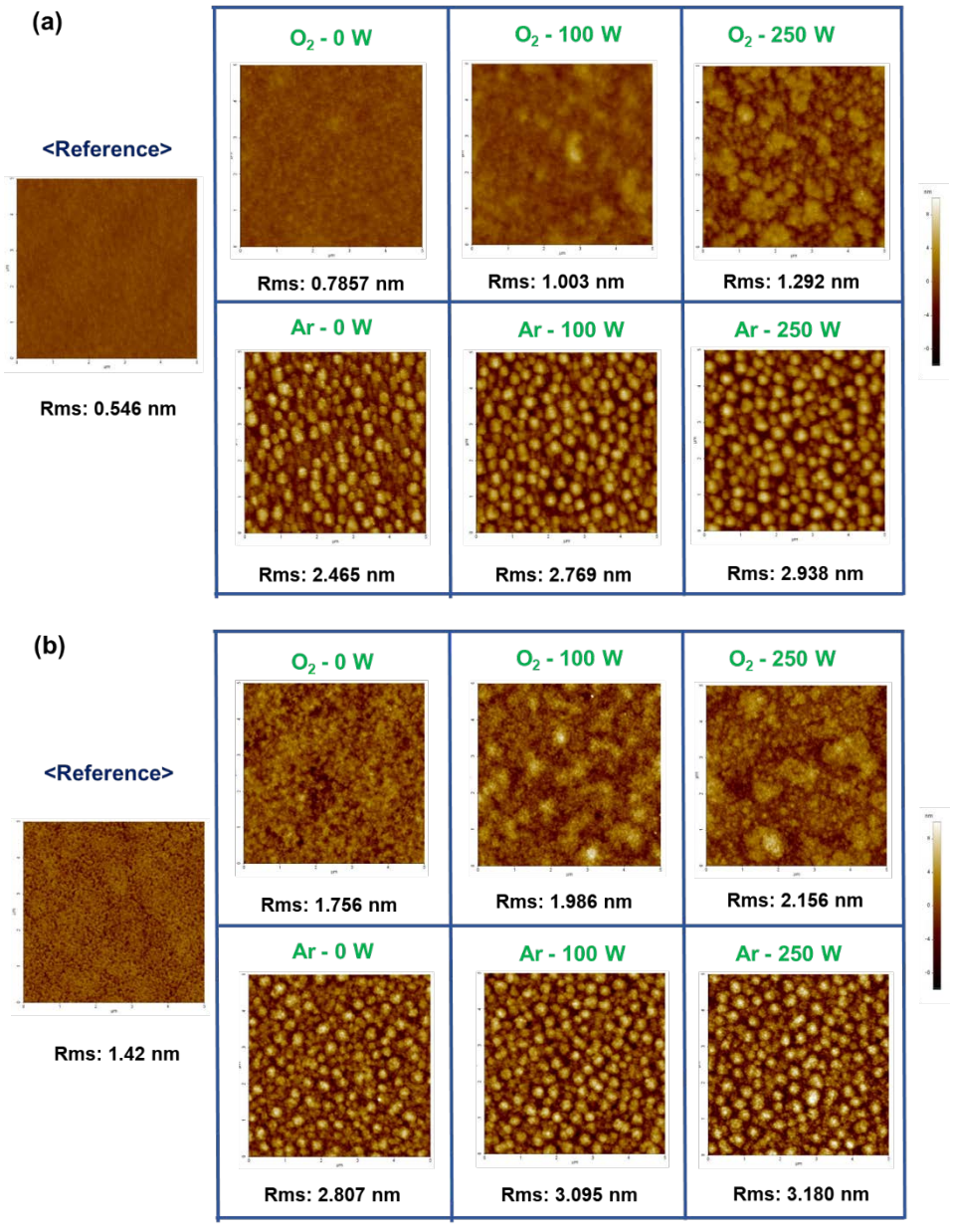

Figure 3.5 2D-AFM images of crystallized alumina (a) gamma-phase (b) alpha-phase

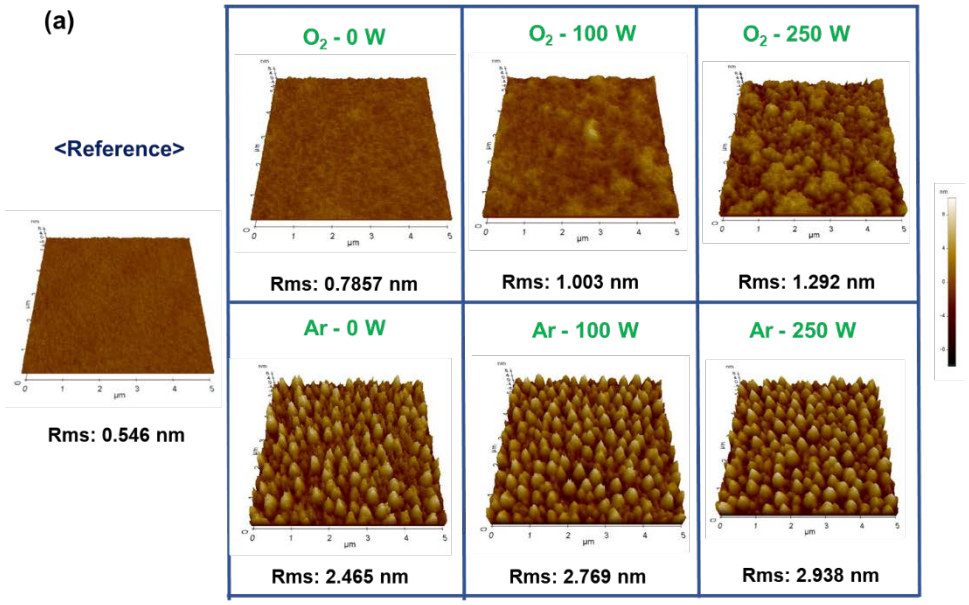

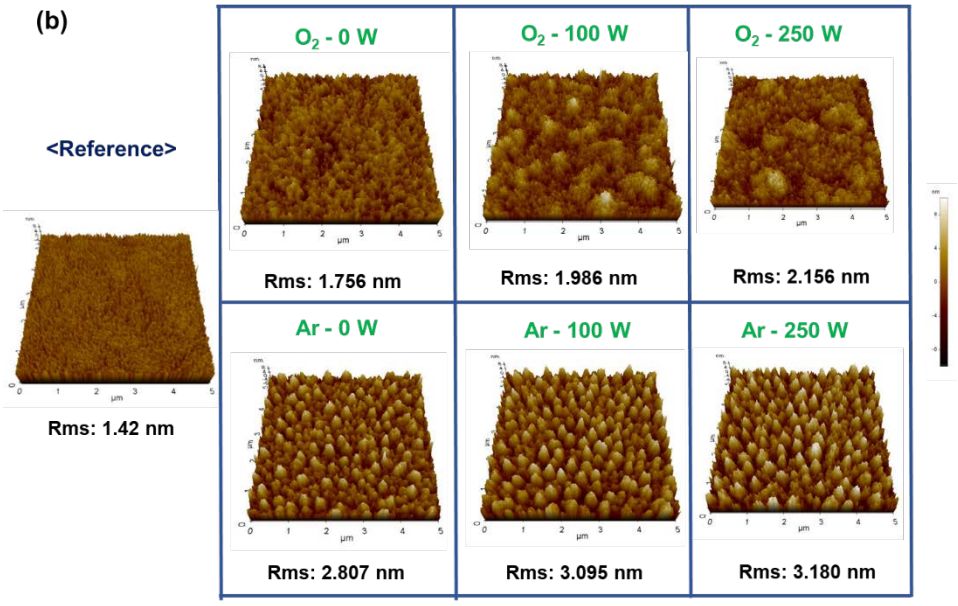

Figure 3.6 3D-AFM images of crystallized alumina (a) gamma-phase (b) alpha-phase

3.2.4 Summary

In this section, analysis of the plasma-treated sapphire surface was studied. To measure the morphology and the roughness, AFM techniques was adopted. In the bare surface and amorphous-phase alumina, there was no significant difference according to plasma treatment. However, unlike the reference, the crystallized samples on the plasma-treated substrate formed nano-size grains and increased roughness. Figure 3.7 shows the summary data of rms roughness. As shown in the figure, roughness of crystallized alumina is increasing by the plate power. It indicates that the greater the plate power, the greater effect on the substrate surface. Also, at the same pate power condition, argon plasma treatment is expected to cause more damage to the substrate than oxygen plasma treatment.

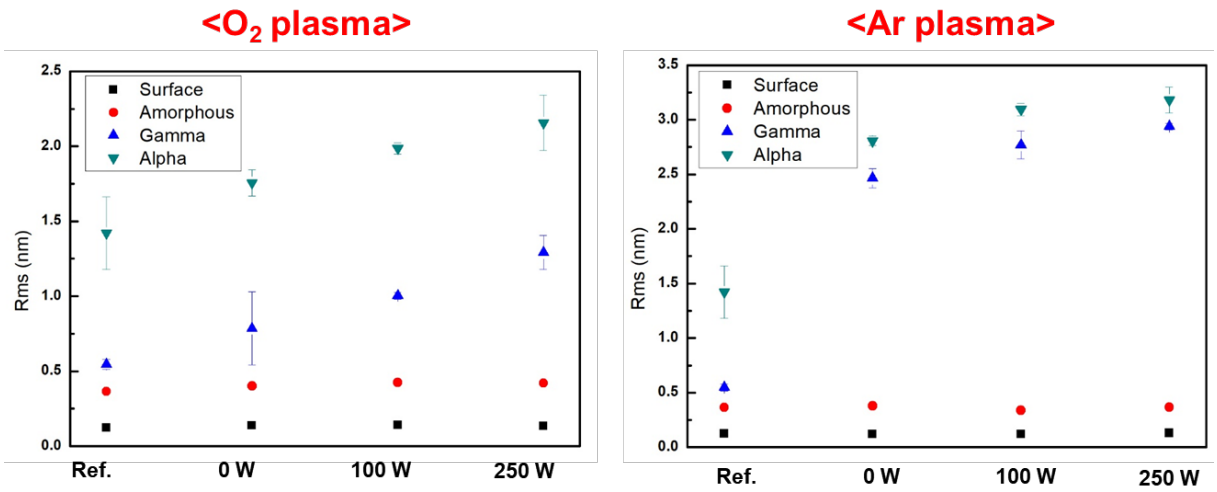

Figure 3.7 RMS roughness depending on the plate power

3.3. XPS analysis (stoichiometry, impurities)

3.3.1 Oxygen plasma treated

In order to investigate the impurities and stoichiometry of alumina surface, chemical binding states were analyzed by XPS technique. As shown in the Figure 3.8 (a), fluorine (F) impurity was found in oxygen plasma treated samples regardless of the plate power. The concentration of fluorine in the total elements detected in XPS spectra (Al, O, C, F) was calculated by CasaXPS program. Fluorine concentration was detected at 10.3% at plate power 0 W, 8.8% at 100 W, 15.2% at 250 W. The ICP-etcher system used in this study uses fluorine-containing gases such as sulfur hexafluoride (SF_6), tetrafluoromethane (CF_4) as well as oxygen and argon. Thus, it can be seen that fluorine was detected by the residual gas remaing in the chamber. Also, the stoichiometry of alumina was examined. Un-treated sapphire substrate had 1.5 of O/Al ratio. When the plate power was 0 W, O/Al ratio was 1.5, which was 1.7 at 100 W and 1.8 at 250 W. It indicates that the higher the plate power, the higher the ratio of oxygen in the alumina surface. This result can be explained by the Oxygen atoms act as interstitial impurities on the sapphire surface. The measured values are summarized in Figure 3.8 (b).

(a)

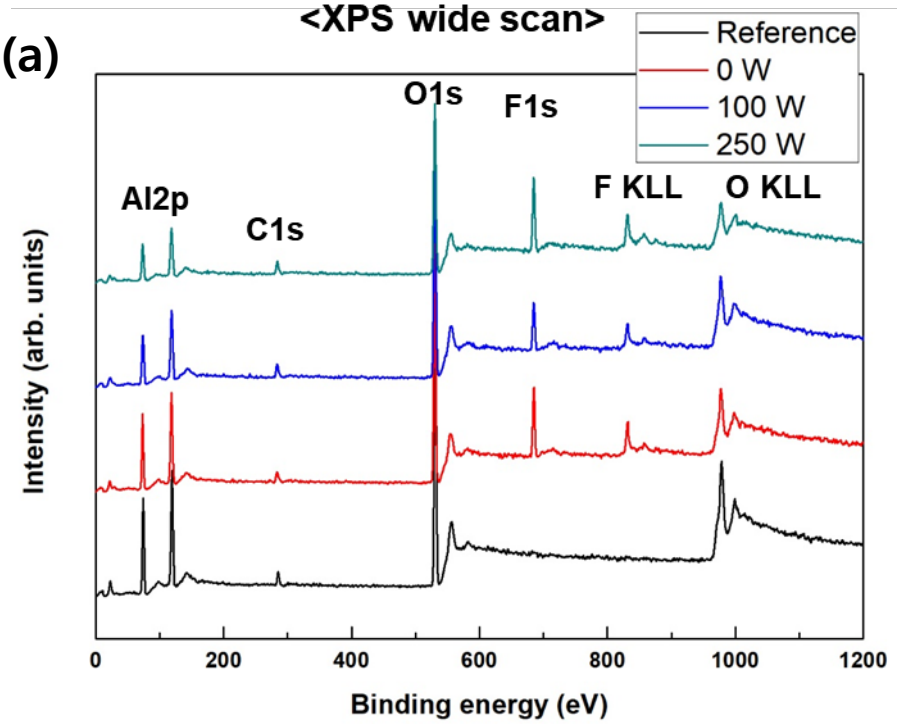

(b)

Sample	Fluorine concentration	O/Al ratio
Reference	-	1.5
0 W	10.3%	1.5
100 W	8.8%	1.7
250 W	15.2%	1.8

Figure 3.8 (a) XPS spectra of oxygen plasma-treated samples (b) table of fluorine concentration and O/Al ratio

3.3.2 Argon plasma-treated

In the case of the argon plasma treatment, surface analysis was examined by XPS. Similar to the result of oxygen plasma treatment samples, a quantity of fluorine was detected. Fluorine concentration was measured at 22.4% at plate power 0 W, 19.0% at 100 W, 15.6% at 250 W. This result indicates that fluorine was detected by the residue gas in the chamber regardless of the plasma gas. Also, a small quanitity of argon is observed at 100 W and 250 W. Argon atoms act as an interstitial impurity on the sapphire surface due to physical collision. The measured value of O/Al ratio shows that the oxygen-deficiency surface was formed by argon plasma treatment. The collision with argon atoms seems to selectively release more oxygen atoms than aluminum atoms. Figure 3.9 (a) exhibits the XPS spectra and figure 3.9 (b) shows the summarized data.

(a)

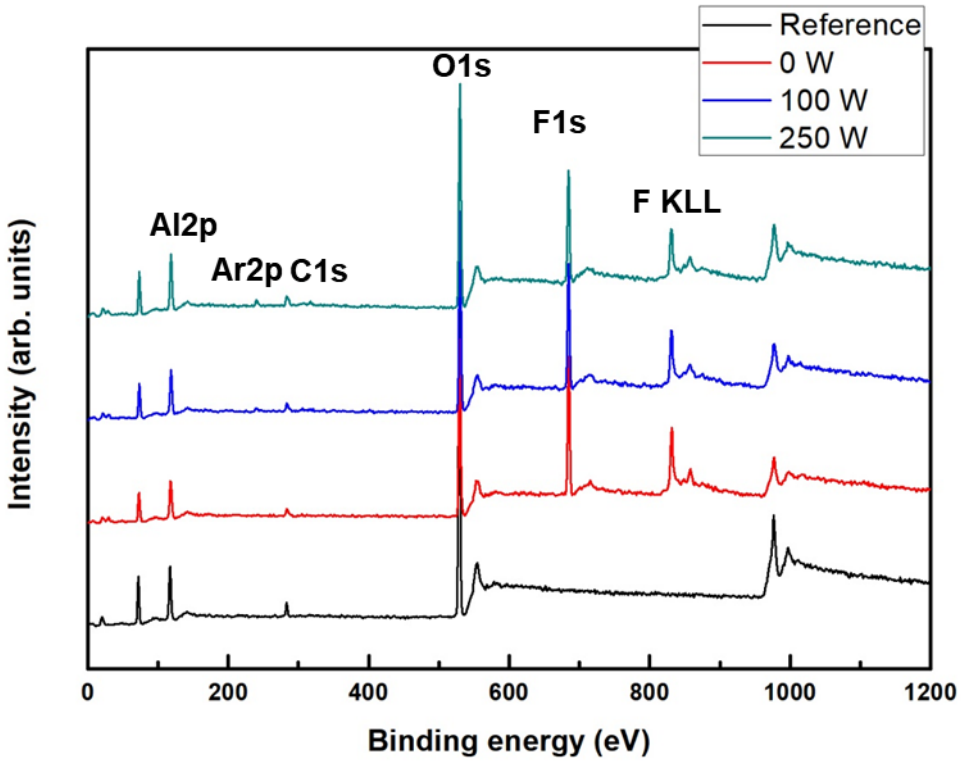

(b)

Sample	Fluorine concentration	Argon concentration	O/Al ratio
Reference	-	-	1.5
0 W	22.4%	-	1.2
100 W	19.0%	0.45%	1.2
250 W	15.6%	0.89%	1.1

Figure 3.9 (a) XPS spectra of argon plasma-treated samples (b) table of fluorine concentration and O/Al ratio

3.3.3 Summary

In this study, XPS technique was used to analyze the stoichiometry of alumina and impurities after plasma treatment. Regardless of the plasma gas, fluorine atoms were detected by residual gas in the chamber. Also, argon atoms were examined in argon plasma treated samples. Compared to O/Al stoichiometry, the oxygen plasma makes the sapphire surface O-rich, while argon plasma O-poor. All the take together, it can be seen that unintended impurity atoms are formed on the surface of the sapphire substrate surface and the stoichiometry is also changed during the plasma treatment process.

3.4. XRD analysis (crystalline quality)

3.4.1 Crystallized gamma-phase alumina

The crystalline quality of crystallized gamma-phase alumina layer on plasma-treated sapphire was analyzed by X-ray diffraction. We measured the ω-rocking curve of gamma-phase alumina (222) plane and obtained the values of FWHM (full width at half maximum). Compared to un-treated sample (reference), all of plasma-treated samples have larger FWHM values, giving about a 21% ~ 34% increment. This results indicate that plasma treatment degraded the crystallinity of the crystallized alumina. This is due to that crystallization processds through SPE process on the sapphire substrate surface where the impurity atoms are generated and the stoichiometry changes during the plasma treatment. Figure 3.10 shows the ω-rocking curve and the FWHM value of each samples.

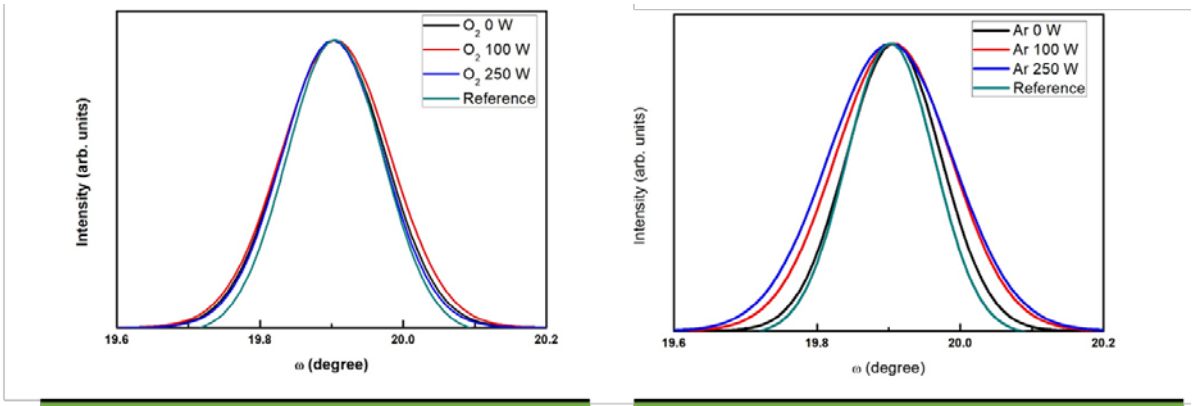

O_2	0 W	100 W	250 W
FWHM (arcsec)	648.7	674.0	638.2

Ar	0 W	100 W	250 W
FWHM (arcsec)	591.7	684.6	718.1

* Reference: 536.7 arcsec

Figure 3.10 ω-rocking curve and FWHM values of crystallized gamma-phase alumina (222) plane

3.4.2 Crystallized alpha-phase alumina

For analysis crystallinity of crystallized alpha-alumina on sapphire substrate, we used reciprocal space mapping (RSM) method. We can get more additional information than single rocking curve scan. ω-scan and 2θ-scan are performed simultaneously to show the information of crystal in three-dimensional. RSM method is increasingly being used to analyze quality in semiconductor materials [22]. Figure 3.11 shows the RSM image ({11-23} plane) of sapphire substrate and crystallized alpha-alumina on plasma-untreated sapphire substrate. As shown in the figure, there is no significant difference in distribution, which means that crystallinity is almost same. However, as shown in Figure 3.12, the distribution of crystallized alpha-alumina on the plasma-treated substrate was found to be broad, which means that crystallinity is degraded. The crystallinity was determined by quantitative analysis and the summarized datas were shown in the table of Figure 3.12. We also measured the crystallinity of CES fabricated using each plasma conditions. However, when the plate power 0 W, in case of both oxygen and argon plasma treatment, surface peeling occurred due to imperfect removal of PR residue. Therefore, these two plasma treatment conditions are not suitable for CES fabrication. Figure 3.13 shows the RSM images of CES and the crystallinity data. As a result, crystallinity of CES was degraded and lower than that of 2-dimensional samples under same plasma conditions.

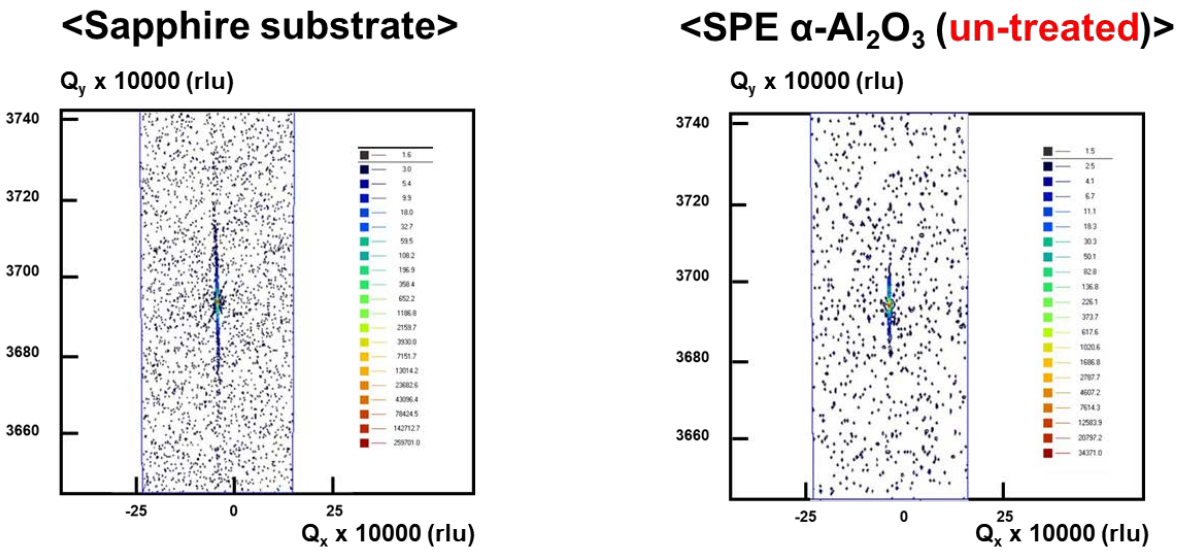

Figure 3.11 RSM images of sapphire substrate and crystallized alpha-alumina on plasma un-treated sapphire substrate.

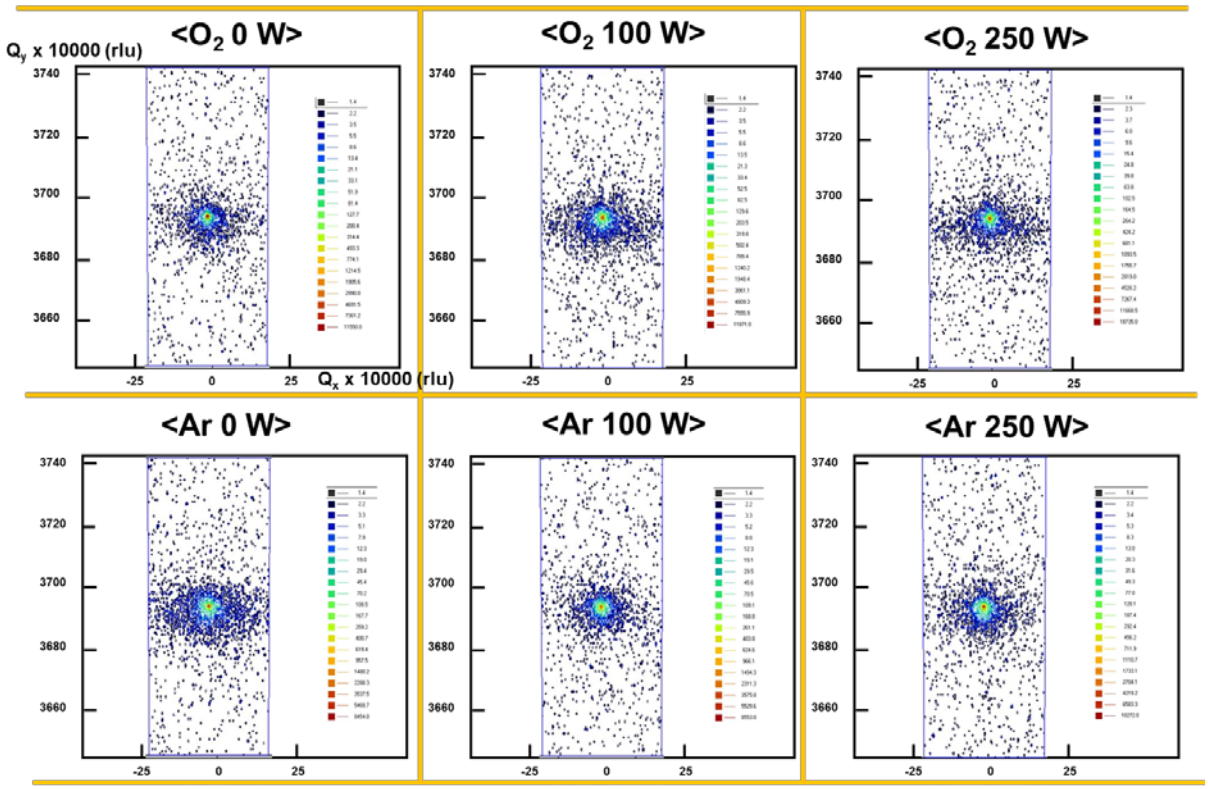

O_2	0 W	100 W	250 W
FWHM (arcsec)	192	228	218

Ar	0 W	100 W	250 W
FWHM (arcsec)	223	225	229

Figure 3.12 RSM images of crystallized alpha-alumina on plasma-treated substrate and the table of summarized FWHM data.

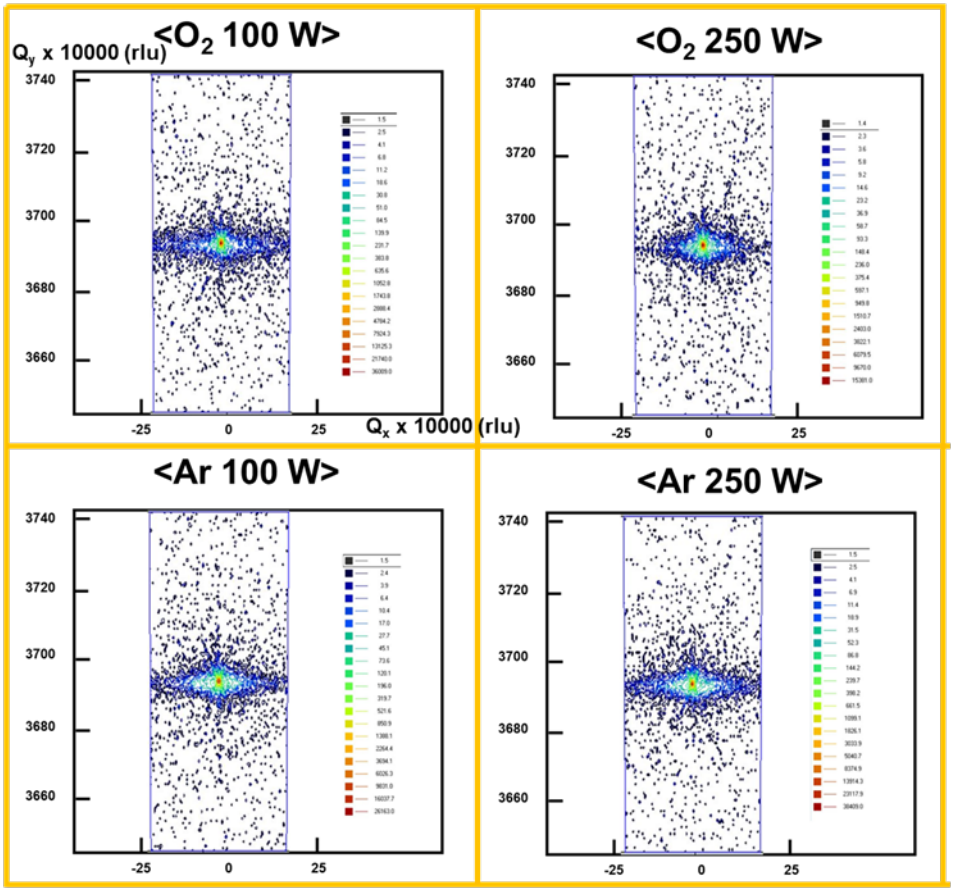

O_2	100 W	250 W
FWHM (arcsec)	258	256

Ar	100 W	250 W
FWHM (arcsec)	263	281

Figure 3.13 RSM images of CES and the table of summarized FWHM data.

3.4.3 Summary

The crystallinity of crystallized alumina was quantitatively analyzed by XRD technique. The plasma treatment of CES fabrication process damages the surface of sapphire substrate and degrades the crystallinity of the crystallized alumina. Through these analysis, it is necessary to find the optimal plasma condition with the best crystallinity of CES.

Chapter 4. Conclusion

To improve the issues of GaN-based LEDs, CES substrate was developed and its effectiveness has been proven through several studies. During the CES fabrication process, plasma processing is an essential step. This study concentrates on analyzing of plasma-treated sapphire substrate and its effect on crystallized alumina quality. As a result, plasma treatment affected the substrate surface and the crystallinity of the crystallized alumina was degraded. Therefore, we need to optimize the plasma treatment to fabricate CES substrate with good crystallinity.

Reference

[1] E.F. Schubert, Light-Emitting Diods. 2nd Edition, Cambridge university press, New York, 2006.

[2] T. Paskova et al., GaN substrates for III-Nitride devices, Proceedings of the IEEE 98, 1324 (2010)

[3] D. Zhu et al., Prospects of III-nitride optoelectronics grown on Si, Reports on Progress Physics 76, 106501 (2013)

[4] D. Cherns et al., Edge and screw dislocations as nonradiative centers in InGaN/GaN quantum well luminescence, Applied Physics Letters 78, 2691 (2001)

[5] H. Y. Shih et al., Ultralow threading dislocation density in GaN epilayer on near-strain-free GaN compliant buffer layer and its applications in hetero-epitaxial LEDs, Scientific Reports 5, 13671 (2015)

[6] A. Usui et al., Thick GaN epitaxial growth with low dislocation density by Hydired vapor phase epitaxy, Japanese Journal of Applied Physics 36, 889 (1997)

[7] Y. Zhonghai et al., Study of the epitaxial-lateral-overgrowth (ELO) process for GaN on sapphire, Journal of Crystal Growth 195, 333 (1998)

[8] Z. Yu et al., Influence of stress in GaN crystals grown by HVPE on MOCVD-GaN/6H-SiC substrate, Scientific Reports 4, 4179 (2014)

[9] Q. Sun et al., GaN-on-Si blue/shite LEDs: epitaxy, chip, and package, Journal of Semiconductors 37, 044006 (2016)

[10] W. Bin et al., Simulation and analysis of GaN wafer bowing on sapphire substrate, Advanced in Condensed Matter Physics 2013, 1 (2013)

[11] J. H. Lee et al., Stress reduction and enhanced extraction efficiency of GaN-based LED grown on cone-shape patterned sapphire, IEEE Photonics Technology Letters 20, 1563 (2008)

[12] C. Y. Cho et al., Growth and separation of high quality GaN epilayer from sapphire substrate by lateral epitaxial overgrowth and wet chemical etching, Applied Physics Express 4, 012104 (2011)

[13] A. I. Zhmakin, Enhancement of light extraction from light emitting diodes, Physics Reports 498, 189 (2011)

[14] J. Kim et al., Less strained and more efficient GaN light-emitting diodes with embedded silica hollow nanospheres, Scientific Reports 3, 3201 (2013)

[15] J. Jang et al., Incorporation of air-cavity into sapphire substrate and its effect on GaN growth and optical properties, Journal of Crystal Growth 430, 41 (2015)

[16] M. A. Herman et al., Epitaxy. 1st edition, Springer, Berlin, 2004.

[17] M. A. Trunov et al., Effect of polymorphic phase transformations in Al_2O_3 film on oxidation kinetics of aluminum powders, Combustion and Flame 140, 310 (2005)

[18] C. W. White et al., Ion implantation and annealing of crystalline oxides and ceramic materials, Nuclear Instruments and Methods in Physics Research B 32, 11 (1988)

[19] G. S. Oehrlein et al., Atomic layer etching at the tipping point: An overview, ECS Journal of Solid State Science and Technology 4, N5041 (2015)

[20] W. J. Park et al., High aspect ratio via etching conditions for deep trench of silicon, Surface and Coatings Technology 171, 290 (2003)

[21] M. D. Groner et al., Low-temperature Al_2O_3 atomic layer deposition, Chemistry of Materials 16, 639 (2004)

[22] P. F. Fewster, Reciprocal space mapping, Critical Reviews in Solid State and Materials Sciences 22, 69 (1997)

국 문 초 록

III-V 족 화합물인 질화갈륨 (GaN) 기반 LED 는 기존의 백열등, 형광등보다 우수한 에너지 효율과 긴 발광 수명으로인해 차세대 조명 기술로 각광받고있다. 일반적으로 질화갈륨 기반 반도체는 사파이어 기판 위에 이종 에피택시 (Hetero-epitaxy) 방법으로 성장시킨다. 하지만 격자상수 차이로 인한 높은 밀도의 관통전위, 열 팽창계수 차이로 인한 기판 휨 현상, 공기와의 높은 굴절률 차이로 인한 낮은 광 추출효율의 문제가 존재한다. 이를 해결하고자 사파이어 기판의 표면에 패턴을 삽입하여 질화갈륨의 측면성장 (Lateral overgrowth)이 가능하게 하고 난반사를 높이는 연구들이 활발하게 진행되고있다. 본 연구실에서도 사파이어 기판위에 빈 공기층을 삽입하는 CES (cavity-engineered sapphire substrate)를 개발하였다. CES 위에 질화갈륨을 성장시킬 경우 측면성장으로 관통전위 밀도가 감소하며 공기층으로 인한 난반사로 인해 광 추출효율이 증가하게 된다. 또한 공기층이 박막내부의 응력을 감소시켜 기판 휨 현상도 완화된다.

CES 는 사파이어 기판에 증착된 비정질-알루미나의 열처리 과정을 이용한 알파-알루미나로의 결정화를 통해 제작한다. 따라서, 고품질의 질화갈륨을 얻기 위해서는 알루미나 층의 결정성이 중요하다고 할 수 있다. CES 제작공정중 비정질-알루미나 층을 증착하기 전 포토리소그래피 공정 후의 감광액 잔여물 제거와 원하는 모양의 패턴을 얻기 위해 플라즈마 처리를 해준다. 이 플라즈마 처리가 사파이어 기판 표면과 추후 기판 위에서 증착된 후 결정화된 알루미나의 결정성에 어떠한 영향을 미치는지 알아보기 위해 본 연구를 진행하였다.

플라즈마 처리는 산소와 아르곤 기체를 이용하여 진행하였으며 각각의 기체에 대하여 기판이 놓이는 판에 인가하는 전력을 조절하여 실험을 진행하였다. 플라즈마 처리후 산소와 아르곤 플라즈마 처리경우 모두 불소 (F) 불순물이 검출되었으며 아르곤 플라즈마 처리 경우에는 소량의 아르곤도 검출되었다. 산소 플라즈마 처리시 사파이어 기판 표면에서 산소가 차지하는 비율이 높아졌으며 아르곤 플라즈마 처리경우에는 반대로, 산소의 비율이 낮아짐을 확인할 수 있었다. 또한 기판이 놓이는 판에인가하는 전력이 커질수록 사파이어 기판 표면의 화학량론이 더 틀어짐을 알 수 있었다. AFM 을 이용한 분석결과 플라즈마 처리시 표면 형상과 거칠기는 달라짐이 크게 없으나 결정화된 시료들의 경우 표면에 나노크기의 결정이 생긴 것을 관찰하였으며 표면 거칠기 또한 크게 증가함을 알 수 있었다. 또한 결정성 분석 결과, 플라즈마 처리 하지 않은 시료들과 비교시 감마-알루미나 와 알파-알루미나의 결정성이 모두 저하됨을 확인할 수 있었다. 따라서 이번연구를 통해 플라즈마 처리가 사파이어 기판 표면과 그 위에서 결정화된 알루미나에 미치는 영향을 실험적으로 규명할 수 있었다.

주요어:

발광 다이오드, 질화갈륨, Cavity-engineered sapphire substrate (CES), 알루미나, 고상에피택시, 플라즈마 처리, 결정성

학번:

2015-20802

Publication list

Conference presentations:

International conference

1. Donghyun Lee, Seungmin Lee, Jeonghwan Jang, Jong-Myeong Kim, **Giwoong Kim**, Jehong Oh, Daeyoung Moon,Yongjo Park and Euijoon Yoon, "Fabrication of nano-cavity patterned sapphire substrates and their application to the growth of GaN", *The 8th Asia-Pacific Workshop on Widegap Semiconductors(APWS-2017)*, September 2017, Qingdao, China.

2. Jeonghwan Jang, Daehan Choi, Seungmin Lee, Daeyoung Moon, **Giwoong Kim**, Duyoung Yang, Jehong Oh, Yongjo Park and Euijoon Yoon, "Epitaxial lateral overgrowth of GaN on partially crystallized cavity engineered sapphire substrate", *The 8th Asia-Pacific Workshop on Widegap Semiconductors(APWS-2017)*, September 2017, Qingdao, China.

3. Donghyun Lee, Seungmin Lee, Jeonghwan Jang, Jong-Myeong Kim, **Giwoong Kim**, Jehong Oh, Daeyoung Moon,Yongjo Park and Euijoon Yoon, "Fabrication of nano-cavity patterned sapphire substrates and their application to the growth of GaN", *The 11th International Symposium on Semiconductor Light Emitting Devices*, October 2017, Banff, Canada.

4. Jeonghwan Jang, Seungmin Lee, Daeyoung Moon, **Giwoong Kim**, Duyoung Yang, Jehong Oh, Yongjo Park and Euijoon Yoon, "Selective area growth of GaN layer on partially

crystallized cavity engineered sapphire substrate", *The 11th International Symposium on Semiconductor Light Emitting Devices*, October 2017, Banff, Canada.

5. Jeonghwan Jang, Daeyoung Moon, **Giwoong Kim**, Duyoung Yang, Yongjo Park and Euijoon Yoon, "Study on solid-phase epitaxy of stripe-shaped Al_2O_3 membrane", *The 11th International Symposium on Semiconductor Light Emitting Devices*, October 2017, Banff, Canada.

6. Euijoon Yoon, Donghyun Lee, Seungmin Lee, Jeonghwan Jang, Jong-Myeong Kim, **Giwoong Kim**, Jehong Oh, and Daeyoung Moon "Fabrication of nano-cavity patterned sapphire substrates and their application to the growth of GaN", *The 4th China-Korea Joint Workshop on Nitride Semiconductors*, October 2017, Chengdu, China.

7. Euijoon Yoon, Donghyun Lee, Seungmin Lee, Jeonghwan Jang, Jong-Myeong Kim, **Giwoong Kim**, Jehong Oh, Daeyoung Moon and Yongjo Park "Fabrication of nano-cavity patterned sapphire substrates and their application to the growth of GaN", *2017 China-Korea Symposium on low dimensional electronic and photonic materials and devices*, November 2017, Shenzhen, China.

Domestic conference

1. 김기웅, 장정환, 문대영, 박용조, 배덕규, 윤의준, “Cavity 패턴 처리된 Sapphire 기판을 통한 광 추출효율 개선”, *제 1 회 LED ・ 반도체조명학회/한국광전자학회 학술대회*, 2015, 대전.

2. 김기웅, 장정환, 문대영, 박용조, 배덕규, 윤의준, “Cavity 패턴 처리된 Sapphire 기판을 통한 광 추출효율 개선”, *한국재료학회 추계학술대회 및 제 29 회 신소재 심포지엄*, 2015, 부산.

3. 김기웅, 장정환, 문대영, 박용조, 배덕규, 윤의준, “Cavity engineered sapphire 기판을 통한 광 추출효율 개선”, *제 2 회 LED ・ 반도체조명학회/한국광전자학회 학술대회*, 2016, 광주.

4. 장정환, 문대영, 김기웅, 박용조, 윤의준, “Incorporation of air-cavity array into GaN layer for high efficient GaN-based LEDs”, *한국결정성장학회 춘계학술대회 및 산업용 단결정/웨이퍼 기술 심층 심포지엄*, 2016, 진주.

5. 김기웅, 장정환, 문대영, 박용조, 윤의준, “Cavity engineered sapphire substrate for high efficiency GaN-based LEDs”, *한국결정성장학회 춘계학술대회 및 산업용 단결정/웨이퍼 기술 심층 심포지엄*, 2016, 진주.

6. 금대명, 김성광, 강항규, 백민, 김기웅, 김상현, 송진동, 최원준, 윤의준, “Re-examination of Fermi level de-pinning for GaSb”, *제 24 회 한국반도체학술대회*, 2017, 홍천.